MISSOURI S&T

Missouri University of Science and Technology

Scholars' Mine

International Specialty Conference on Cold-Formed Steel Structures

(1988) - 9th International Specialty Conference on Cold-Formed Steel Structures

Nov 8th, 12:00 AM

Nonlinear Analysis of Cold-formed Sections Using the Finite Strip Method

Peter W. Key

Gregory J. Hancock

Follow this and additional works at: https://scholarsmine.mst.edu/isccss

Part of the Structural Engineering Commons

Recommended Citation

Key, Peter W. and Hancock, Gregory J., "Nonlinear Analysis of Cold-formed Sections Using the Finite Strip Method" (1988). *International Specialty Conference on Cold-Formed Steel Structures*. 4.
https://scholarsmine.mst.edu/isccss/9iccfss-session1/9iccfss-session1/4

NONLINEAR ANALYSIS OF COLD-FORMED SECTIONS USING THE FINITE STRIP METHOD

by

Peter W. Key[1] and Gregory J. Hancock[2]

Summary

A large deflection elastic-plastic analysis has been developed using the finite strip method to determine the inelastic postbuckling behaviour of cold-formed sections in compression. The analysis accounts for plate geometric imperfections, the variation of yield stress around a section, the stress-strain characteristics of the material forming the section and the highly complex patterns of residual stress produced by the cold-forming process.

The analysis is compared with the results of compression tests performed at the University of Sydney on stub columns of cold-formed hollow sections. An important part of the testing programme was the measurement of residual stress through the plate thickness of the cold-formed hollow sections. The effect of this through thickness residual stress on the compression and local buckling behaviour of the cold-formed sections is demonstrated using the finite strip analysis.

[1] Postgraduate Student, School of Civil and Mining Engineering, University of Sydney, Australia

[2] Associate Professor, School of Civil and Mining Engineering, University of Sydney, Australia

1. INTRODUCTION

The increasing use of thin–walled structural steel sections, together with the current or pending revision of many steel structures codes and specifications to limit state format, has led to an increased interest in the ultimate strength and post–ultimate behaviour of thin–walled sections. Fundamental to the assessment of ultimate load capacity is the ability to reliably predict the cross–sectional load–deformation response, taking into account local buckling, initial geometric imperfections in the section, residual stresses produced by manufacturing processes and material yielding. This paper outlines the development of a computationally efficient yet rigorous material and geometric nonlinear analysis for the above problem based on the finite strip method of analysis (Cheung 1976). The results are verified against solutions for a variety of problems of plates and sections under axial compression.

Graves–Smith (1967) is credited with producing the first load–shortening curves for steel plates taking into account both large deflections and plasticity. The analysis used a Rayleigh–Ritz approach and assumed a linear stress distribution through the plate thickness but did not allow for elastic unloading from the yield surface. Moxham (1970, 1971) and Little (1977) produced further developments of this technique with improvements in the stress distribution through the thickness of the plate and improved numerical procedures. Crisfield (1973), Frieze et al. (1977) and Harding et al. (1977) produced similar analyses based on the finite element and finite difference methods.

The finite strip method was first applied to the elastic postbuckling analysis of plate assemblies by Graves–Smith and Sridharan (1978) and to the nonlinear analysis of plate assemblies by Hancock (1981). Mofflin (1983) adopted Little's (1977) energy formulation in a nonlinear finite strip analysis incorporating plasticity to study the behaviour of stiffened plates and sections composed of both steel and aluminium. The method described in this paper is similar to Mofflin's analysis in that it uses the finite strip method. However, the solution procedure is based on the Newton–Raphson procedure rather than the live energy method described by Little.

In an earlier paper (Key, Hasan and Hancock 1988), the results of compression tests on Australian produced cold–formed rectangular and square hollow sections (SHS) were described. The material stress–strain relationships and the variation of yield stress around the cold–formed tubes were described in the paper. Distributions of surface residual stress were also measured and described in the paper. A sample of Australian produced cold–formed square hollow section was sent to Cambridge University, U.K. where the through thickness residual stress distribution was determined using a spark erosion technique (Scaramangas 1984). The measured through thickness residual stress distribution has been incorporated within the nonlinear finite strip analysis described in the paper. The influence of the through thickness residual stresses on the cold–formed section capacity is determined analytically and compared with the test results of the thinner sections.

2. NONLINEAR ANALYSIS

2.1 General

The finite strip procedure, in which a prismatic member is discretised into a number of strips which are joined at longitudinal nodal lines as shown in Fig. 1, is a modification of the more general finite element technique While the finite element technique uses polynomial displacement functions in both directions, the

finite strip procedure uses a continuously differentiable smooth series (typically a Fourier series) in the longitudinal direction and a relatively simple polynomial function in the transverse direction. The longitudinal functions are chosen to satisfy the end boundary conditions and the transverse polynomial functions normally give compatibility between strips. For buckling of thin-walled sections, the longitudinal functions are normally harmonic and match the longitudinal variation of the buckling modes as derived from an analytical buckling solution. Hence the method is sometimes called the "semi-analytical finite strip method".

Under the action of compressive load, a thin-walled prismatic plate assembly may locally buckle into a number of half-waves between nodal planes as depicted in Fig. 2. The length of section between nodal planes and equal to a half-wavelength has been called a "locally buckled cell" in this paper. Each locally buckled cell can be analysed independently and the behaviour of the full member modelled as a synthesis of the locally buckled cells as described by Davids and Hancock (1987).

The finite strip analysis described in this paper divides a locally buckled cell into a number of strips longitudinally. The boundary conditions at the nodal planes of a local buckle are assumed to be:

(a) no in-plane shear strain.

(b) the cross-section remains undistorted implying no flexural displacements.

(c) plate flexural moments are unrestrained.

(d) no longitudinal displacements.

2.2 Displacement Functions

A typical strip and adopted coordinate system are shown in Fig. 3. The strip is assumed to be bent and compressed between rigid frictionless platens which produce applied strains ϵ_1 and ϵ_2 on nodal lines 1 and 2 respectively. The resulting total displacements are given by:

$$u = u_H + u_P + u_S \tag{1a}$$

$$v = v_H + v_P + v_S \tag{1b}$$

$$w = w_P + w_S \tag{1c}$$

where subscript 'H' refers to the prebuckling (Hookean) displacements, and the subscripts 'P' and 'S' refer to primary and secondary deformations. The membrane displacements corresponding to the Hookean deformations are given by (see Fig. 3),

$$u_H = (\rho y - \epsilon_1)(x - L/2) \tag{2a}$$

$$v_H = v_R + \nu(\epsilon_1 y - \rho y^2/2) + \rho x(L - x)/2 \tag{2b}$$

where $\rho = (\epsilon_1 - \epsilon_2)/b$ and v_R is a rigid body displacement

The primary (buckling) displacements are given by:

$$u_P = \Sigma\ f_u(n)\ \cos(n\pi x/L) \tag{3a}$$

$$v_P = \Sigma\ f_v(n)\ \sin(n\pi x/L) \tag{3b}$$

$$w_P = \Sigma\ (f_w(n)\ \sin(n\pi x/L) - f_{0w}(n)\ \sin(n\pi x/L)) \tag{3c}$$

for n = 1,3,5,7, ...

where $f_u(n)$, $f_v(n)$ are linear functions of y alone and $f_w(n)$ is a cubic function of y alone. $f_{0w}(n)$ is a cubic function of y alone describing the initial imperfection.

The secondary (postbuckling) displacements are given by:

$$u_S = \Sigma\ f_u(m)\ \sin(m\pi x/L) \tag{4a}$$

$$v_S = \Sigma\ f_v(m)\ \cos(m\pi x/L) \tag{4b}$$

$$w_S = \Sigma\ (f_w(m)\ \cos(m\pi x/L) - f_{0w}(m)\ \cos(m\pi x/L)) \tag{4c}$$

for m = 0,2,4,6,...

where $f_u(m)$, $f_v(m)$ are linear functions of y alone and $f_w(m)$ is a cubic function of y alone. $f_{0w}(m)$ is a cubic function of y alone describing the initial imperfection.

Sridharan and Graves–Smith (1981) have shown that if n=1 is selected for the primary displacements, then m=0,2 should be used for the secondary displacements. Sridharan (1982) developed the full set of Equations 1–3 for buckling modes of thin–walled sections which include both flexural and membrane deformations in the primary mode. The finite strip post–local buckling analysis described by Graves–Smith and Sridharan (1978) and the nonlinear analysis described by Hancock (1985) employ a subset of Equations 3 and 4 given by Equations 4a, 4b describing membrane deformations and Equation 3c describing flexural deformations. The subset satisfies the end boundary conditions summarised in Section 2.1 and has been used in the analysis described in this paper. The boundary conditions at plate junctions are not completely compatible and have been summarised in detail in Hancock (1985).

2.3 Strain–Displacement Relations

The strain–displacement equations relate the strain state at any position in the plate to the displacement fields given by Equations 1 – 4. In the context of the present analysis, account has been taken of finite flexural displacements only. The strains in the plate at mid–thickness are therefore given by:

$$_m\epsilon_x = \frac{\partial u}{\partial x} + \left[\frac{1}{2}\left[\frac{\partial w}{\partial x}\right]^2 - \frac{1}{2}\left[\frac{\partial w_0}{\partial x}\right]^2\right] \tag{5a}$$

$$_m\epsilon_y = \frac{\partial v}{\partial y} + \left[\frac{1}{2}\left[\frac{\partial w}{\partial y}\right]^2 - \frac{1}{2}\left[\frac{\partial w_0}{\partial y}\right]^2\right] \tag{5b}$$

$$_m\gamma_{xy} = \frac{\partial u}{\partial y} + \frac{\partial v}{\partial x} + \left[\frac{\partial w}{\partial y}\cdot\frac{\partial w}{\partial x} - \frac{\partial w_0}{\partial y}\cdot\frac{\partial w_0}{\partial x}\right] \tag{5c}$$

where w_0 is the initial plate imperfection. It is assumed that normals to the surface remain straight and perpendicular to the deformed middle surface so that the strains at any point x,y,z are given by:

$$\epsilon_x = {}_m\epsilon_x - z \frac{\partial^2 (w - w_0)}{\partial x^2} \qquad (6a)$$

$$\epsilon_y = {}_m\epsilon_y - z \frac{\partial^2 (w - w_0)}{\partial y^2} \qquad (6b)$$

$$\gamma_{xy} = {}_m\gamma_{xy} - z \frac{\partial^2 (w - w_0)}{\partial x\, \partial y} \qquad (6c)$$

2.4 Stress–Strain Relations

An increment of strain is in general composed of an elastic component and a plastic component. Up to the point of yield, strain increments are entirely elastic and the stress is related to strain through the conventional elastic constitutive relationships given by Timoshenko and Woinowsky–Krieger (1959). Once yielding begins, the Prandtl–Reuss flow rule (Mendelson 1968), given by Equation 7, governs the proportion of the total strain increment that occurs plastically.

$$\frac{\Delta\epsilon_x^p}{S_x} = \frac{\Delta\epsilon_y^p}{S_y} = \frac{\Delta\gamma_{xy}^p}{S_{xy}} = \lambda \qquad (7)$$

where λ is a positive scalar, $S_x = \sigma_x - \sigma_m$, $S_y = \sigma_y - \sigma_m$ and $S_{xy} = 2\tau_{xy}$

$$\sigma_m = \left[\frac{\sigma_x + \sigma_y + \sigma_z}{3} \right] \qquad (8)$$

The normal stress σ_z is assumed to be zero. The von Mises yield criterion (Mendelson 1968) given by Equation 9 is used to relate yield occurring under a state of biaxial stress to the yield stress in simple tension or compression.

$$\sigma_e = \left[\sigma_x^2 + \sigma_y^2 - \sigma_x\sigma_y + 3\tau_{xy}^2 \right]^{\frac{1}{2}} \qquad (9)$$

Yielding will begin when the von Mises effective stress σ_e reaches the uniaxial yield stress. The plasticity model adopted assumes the yield stress is equal in tension and compression and the material strain hardens isotropically.

2.5 Equilibrium Equations

The total equilibrium equation provides a relation between the stress state in a strip and its current deformed shape. The principle of virtual displacements, which is applicable irrespective of the material behaviour, can be used to formulate the total equilibrium equation (Equation 10) in terms of the strip nodal line displacements.

$$\int_V d\epsilon_i\, \sigma_i\, dV = \left\{ d\delta \right\}^T \left\{ W \right\} \qquad (10)$$

where the repeated indices imply summation. The σ_i are the components σ_x, σ_y, τ_{xy} of the internal stress distribution in equilibrium with the external load system $\{W\}$ and the $d\epsilon_i$ are the variations in the strain components ϵ_x, ϵ_y, γ_{xy} resulting from the virtual nodal line displacements $\{d\delta\}$. The strain ϵ_i and its increment $d\epsilon_i$ can be expressed as a function of the nodal line displacements using Equations 1 – 6. As a consequence of plasticity, the current stress state σ_i at any point within the strip is a function of the strain history at that particular location and cannot be uniquely defined in terms of the total strain. The elastic–plastic stress–strain relations are used to update the current stress as increments of load are applied.

The solution procedure for the total equilibrium equation requires a relationship between the increments of applied load and the resultant incremental displacements, valid for the current material and deformation state of the structure. If two neighbouring equilibrium states are considered, each of which can be expressed in the form of Equation 10, the difference between the two yields the incremental equilibrium equation, given by Equation 11.

$$\left[\; k_T \; \right] \; \left\{ \; \Delta\delta \; \right\} = \left\{ \; \Delta w \; \right\} \qquad\qquad (11)$$

$[k_T]$ is the tangent stiffness matrix for a single strip in the local coordinate system and relates the increment of nodal load $\{\Delta w\}$ to the resultant incremental displacement $\{\Delta\delta\}$. The total and incremental equilibrium equations, evaluated for a strip in its local x,y,z coordinate system, must be transformed to the global axis system X,Y,Z when assembling the tangent stiffness matrix $[K_T]$ for the whole section.

2.6 Solution Procedure

The combined material and geometric nonlinear finite strip analysis detailed in this paper uses a modified Newton–Raphson solution procedure in which the tangent stiffness matrix is updated at the beginning of the load increment and also at stages during the iteration procedure, depending on the rate of convergence or possible divergence. Equilibrium is checked using Equation 10, which calculates an out–of–balance load vector for subsequent use with the tangent stiffness equations to estimate incremental deflection. Convergence is firstly achieved based on a fixed level of plasticity. The yield criterion is then checked and adjustments made to the stresses which have reached yield during the current increment, exceeded the stress on the yield surface or elastically unloaded from the yield surface. Equilibrium is reestablished using the Newton–Raphson procedure and the process repeated until the convergence criteria are satisfied.

As a consequence of the path dependent nature of the flow rules of plasticity, the three stresses σ_x, σ_y and τ_{xy}, and the Von Mises effective stress σ_e are stored at each monitoring point shown in Fig. 4. Integration is performed longitudinally in each strip using Gaussian quadrature to obtain maximum efficiency from a minimum number of monitoring stations (shown as n_2 in Fig. 4). Laterally, integration is performed using simple summation with n_1 monitoring stations while Simpson's rule integration is used through the thickness with n_3 layer points as shown in Fig. 4.

3. INVESTIGATION OF PROGRAM PARAMETERS AND ACCURACY

3.1 Parameters

A number of parameters in the program required investigation to establish suitable values for accurate analyses. These were:

(a) Number of lateral monitoring stations (n_1)

(b) Number of longitudinal monitoring stations (n_2)

(c) Number of layer points (n_3)

(d) Number of Fourier terms (n,m)

A simply supported square plate with edges free to pull in and an initial imperfection of $w_0/t = 0.1$ in the buckling mode was chosen to investigate the influence of the above parameters on the load–displacement behaviour. Utilising symmetry, 3 strips were used over a half–width of plate. The results are graphed in Fig. 5(a)–(d) as non–dimensionalised stress (σ_m/σ_{cr}) versus non–dimensionalised central deflection (w/t), where σ_m is the mean longitudinal compressive stress in the plate and σ_{cr} is the elastic buckling stress for the square plate. Both elastic and elastic–perfectly plastic material behaviour have been investigated such that the yield stress σ_y is equal to the elastic buckling stress σ_{cr}. It is generally accepted that the solution of Yamaki (1959) for the purely elastic case gives an accurate representation of plate behaviour up to 3 times the buckling strain and this solution is also shown in Fig. 5. A summary of the results is as follows:

(a) The difference in ultimate load for the cases of two and four lateral monitoring stations per strip was 0.07 percent. Generally two lateral monitoring stations per strip were adopted for all analyses.

(b) A comparison between the cases of 3 and 6 longitudinal monitoring stations over half of the strip length gave a difference in ultimate load of approximately 0.05 percent. As a consequence of longitudinal symmetry, only half of the length of the strips were integrated and generally 6 monitoring stations per half strip were adopted for all subsequent calculations.

(c) For the elastic case, 3 layer points were sufficient to describe the through thickness variation. For the elastic–plastic case, 5 layer points were necessary.

(d) In advanced stages of elastic postbuckling, change of waveform can occur. Hence additional terms (n=3, m=4,6) are required in the Fourier analysis to describe the change of waveform. However, for elastic–plastic analyses of sections for which yielding and buckling occur approximately simultaneously, the additional Fourier terms gave no practical difference in ultimate load. The n=1, m=0,2 Fourier set was generally adopted for all subsequent investigations.

3.2 Numerical Study of a Single Plate

Plate load–shortening curves predicted by the finite strip nonlinear analysis have been compared in Fig. 6 with the results predicted by Moxham (1971), Little (1977), Frieze et al. (1977) and Harding et al. (1977). The material behaviour was elastic–perfectly plastic. Four levels of plate slenderness (b/t) were analysed

ranging from values of 30 to 80. The aspect ratio of the plate was taken as a/b = 7/8 being that adopted by the other researchers and found to give the minimum ultimate load. The case shown is for a residual stress free plate with a small initial geometric imperfection of $w_0/b = 0.001$. Three strips over half of the plate were found to produce ultimate loads within 0.16 percent of the value when 8 strips were used over half of the plate. Consequently 3 strips were adopted in the analysis.

The present finite strip solution compares favourably with the results of Little. The significant variation between results predicted by the various researchers is mainly a function of the plasticity model adopted, especially the use of the full section yield criterion by Harding et al. and Frieze et al. Little's method modelled through thickness plasticity using a layer approach and took full account of elastic unloading.

3.3 Numerical Study of a Fabricated Box Section

The present finite strip solution has been compared with Mofflin's (1983) results for a square box section at different plate slenderness values. Four strips over each face of a symmetric quarter box were used in the analysis. The material behaviour was modelled as elastic–perfectly plastic. The ultimate strengths are given in Fig. 7 and agree well with the results of Mofflin which included a sympathetic geometric imperfection of magnitude $w_0/b = 0.005$ and no residual stress. The effect of an imperfection where the deflection of the plates is opposite to the buckling mode (called "adverse imperfection") is to substantially increase the strength of the section as shown in Fig. 7.

4. COMPARISON OF THEORY WITH TESTS OF COLD–FORMED SQUARE HOLLOW SECTIONS

4.1 Residual Stresses

Two distinct sets of residual stress measurements were made on the test sections described in Key, Hasan and Hancock (1988). These were:

(a) A spark erosion technique (Scaramangas 1984) was used on a section of plate cut from a 254×254×6.3mm SHS to measure the through thickness variation of residual stress in both the longitudinal and transverse directions at the centre of a face. The results of these measurements are summarised in Fig. 8.

(b) Longitudinal released surface strains were measured around a section of 152×152×4.9mm SHS using the sectioning technique. The results of this investigation are fully described in Key, Hasan and Hancock (1988).

The released residual stresses resulting from panel removal as part of (a) above are shown in Fig. 8(a). These longitudinal stresses are tensile on the outside and compressive on the inside, whereas the transverse residual stresses are compressive on the outside and tensile on the inside. The released residual stresses resulting from small block removal from the panel are shown in Fig. 8(b). These stresses are small compared with the panel removal stresses. The through thickness variation of the panel removal and block removal stresses is assumed to be linear according to engineering bending theory. The released residual stresses obtained from the spark erosion layering process of the small block are shown in Fig. 8(c). Two measurements were taken of both the longitudinal and transverse variation as shown in Fig. 8(c). The layering stresses were found to have magnitudes

comparable with the panel removal values.

The longitudinal released surface strains described in (b) above are the same component as the sum of the panel removal and block removal values described in (a) above, except that in (b), measurements have only been taken in the longitudinal direction. The variation in the transverse direction was not measured but was taken from those reported by Kato (1982) and Kato et al. (1986) which indicated that the transverse residual stress could be considered uniform across the section face. For the purpose of the analyses, it was assumed that the distribution described in (b) was applicable to all four section sizes of square hollow section described in Key, Hasan and Hancock (1988). The analytical models of the distribution of membrane and bending residual stress around the section and adopted in the finite strip analysis are shown in Figs. 9, 10 and 11.

The experimentally measured residual stress distributions on the 254×254×6.3 SHS were reduced to analytical models for inclusion in the finite strip analysis. The following steps were taken to model the residual stress distribution.

(a) The panel removal stress was modelled as a membrane component and a bending component, as shown in Fig. 10.

(b) The released residual stress determined from small block removal was found to be negligible compared with the panel removal stress and so was ignored in the analyses.

(c) The released residual stress determined from layering was modelled as shown in Fig. 11. The models satisfy the equilibrium requirements of zero nett axial force and moment. Thirteen layer points were used in the finite strip analysis to adequately model the residual stress distribution through the thickness. These layer points, labelled P_1 to P_{13}, are also shown in Figs. 10 and 11.

The final residual stress distributions adopted in the finite strip analysis for the cold-formed SHS were:

(a) Longitudinal membrane component $\chi\sigma_R$ where σ_R is 30 MPa and χ is the distribution on each face given by Fig. 9(a).

(b) Longitudinal bending component given by $\chi\sigma_R$ where σ_R is the bending analytical variation in Fig. 10(a) and χ is the distribution on each face given by Fig. 9(b).

(c) Longitudinal layering component given by $\chi\sigma_R$ where σ_R is the analytical layering variation in Fig. 11(a) and χ is the distribution on each face given by Fig. 9(c).

(d) Transverse membrane component is zero.

(e) Transverse bending component given by $\chi\sigma_R$ where σ_R is the bending analytical variation in Fig. 10(b) and χ is the distribution on each face given by Fig. 9(e).

(f) Transverse layering component given by $\chi\sigma_R$ where σ_R is the analytical layering variation in Fig. 11(b) and χ is the distribution on each face given by Fig. 9(f).

The longitudinal membrane component $\chi\sigma_R$ has been based on the values measured in the 152×152×4.9 SHS. Similarly, the longitudinal bending component has also been based on the values in the 152×152×4.9 SHS. Since the values in Fig. 10(a) are those determined for the 254×254×6.3 SHS, then a maximum value of the χ factor based on the ratio of the maximum longitudinal bending stress measured in the 152×152×4.9 SHS (200 MPa) to that in the 254×254×6.3 SHS (250 MPa) has been used. This produces a maximum value of χ equal to 0.8. The longitudinal and transverse layering components and transverse bending components have been based on the 254×254×6.3 SHS measurements but factored by the same value of χ as used for the longitudinal bending component.

Within the analysis, the stresses resulting from applied load were added to the residual stresses before application of the von Mises yield criterion (Equation 9).

4.2 Geometric Model and Stress–Strain Characteristics

The cold–formed sections were analysed over a length equal to 0.8 times the elastic buckling half–wavelength. This value was found from analytical studies to produce the minimum ultimate load. The section was modelled as quarter of a box between the centrelines of adjacent faces. Each half face was modelled using 5 coplanar strips with the 5th strip narrower than the other four and representing the corners of the section with enhanced yield strength and a rounded stress–strain curve. The stress–strain curves used were modelled analytically from those described in Key, Hasan and Hancock (1988). The geometric imperfections were taken as $w_0/b = 0.001$ in the adverse mode as described in Section 3.3, since the imperfections in the tests specimens were observed to be in this shape.

4.3 Numerical Studies

The finite strip analysis with thirteen layer points through the plate thickness was used to investigate the nonlinear response of the four SHS sections described in Key, Hasan and Hancock (1988). The influence of the various components of residual stress was investigated by progressive inclusion of the components in the analysis. The average stress versus axial strain has been plotted for the 254×254×6.3 SHS in Fig. 12. Results have been non–dimensionalised with respect to the nominal yield stress (σ_Y) of 350 MPa and the corresponding yield strain ϵ_Y. These graphs are typical of those for all four sections.

The influence of the different components of the residual stress is quite clear in the figure. In particular, the longitudinal bending component of residual stress and the total transverse residual stresses each have a significant influence on the nonlinear behaviour of the section. The curve including all components of residual stress is quite close to the experimentally measured curve and justifies the care taken to include all components of residual stress in the analysis.

5. CONCLUSIONS

A detailed description of a finite strip method for the nonlinear analysis of thin-walled and cold-formed steel sections has been described. The analysis accounts for geometric nonlinearity and material plasticity in the behaviour of sections subjected to axial compression and undergoing inelastic local buckling deformations.

The analysis includes the effects of geometric imperfections, yield stress variation and complex patterns of residual stress produced by the cold-forming process. The accuracy of the analysis was tested against reliable solutions for plates in compression and a fabricated box section.

A description was given of residual stresses measured in a cold-formed SHS after manufacture. The stress distributions included the variations through the thickness of the steel in both the longitudinal and transverse directions. A comparison of the nonlinear finite strip model including all components of residual stress with the test results for a cold-formed tube demonstrated close agreement in the load-shortening response up to ultimate. In addition, analyses which included the different components of residual stress in isolation demonstrated the importance of several components including the transverse components of residual stress. The program will be a useful tool for further studies on the effects of residual stress, geometric imperfections, material behaviour and plate slenderness on the strength of cold-formed sections.

6. ACKNOWLEDGEMENTS

7. APPENDIX I REFERENCES

Cheung, Y.K. (1976), Finite Strip Method in Structural Analysis, Pergamon Press, Inc., New York, NY.

Crisfield, M.A. (1973), "Large Deflection Elastic-Plastic Buckling Analysis of Plates using Finite Elements", Transport and Road Research Laboratory Report, LR593, Dept of Environment, England.

Davids, A.J. and Hancock, G.J. (1987), "Nonlinear Elastic Response of Locally Buckled Thin-Walled Beam-Columns", Thin-Walled Structures, Vol.5, No. 3 pp 211-226.

Frieze, P.A., Dowling, P.J. and Hobbs, R.E. (1977), "Ultimate Load Behaviour of Plates in Compression", Steel Plated Structures, Crosby Lockwood Staples, London.

Graves-Smith, T.R. (1967), "The Ultimate Strength of Locally Buckled Columns of Arbitrary Length", Thin-Walled Steel Structures, Edited by Rockey and Hill, Crosby Lockwood and Son, London.

Graves-Smith, T.R. and Sridharan, S. (1978), "A Finite Strip Method for the Post-Locally Buckled Analysis of Plate Structures", Int. J. Mech. Sci., Vol. 20, pp 833-842.

Hancock, G.J. (1981), "Nonlinear Analysis of Thin Sections in Compression", Jour. Struct. Div., ASCE, Vol. 107, No. ST3, March, pp 455-471.

Hancock, G.J. (1985), "Nonlinear Analysis of Thin–Walled I–Sections in Bending", Chapter 14 of Aspects of the Analysis of Plate Structures, Ed. D.J. Dawe, R.W. Horsington, A.G. Kamtekar, and G.H. Little, Oxford University Press.

Harding, J.E., Hobbs, R.E. and Neal, B.J. (1977), "The Elastic–Plastic Analysis of Imperfect Square Plates under In–Plane Loading", Proc. Inst. Civ. Engrs., Part 2, Volume 63, pp137–158.

Kato, B. (1982), " Cold–Formed Welded Steel Tubular Members", Chapter 5 of Axially Compressed Structures, Ed. R. Narayanan, Applied Science Publishers, London and New York.

Kato, B. and Narihara, H. (1986), " Residual Stresses in Square Steel Tubes Introduced by Cold–Forming and the Influence on Mechanical Properties", Proceedings, International Meeting on Safety Criteria in the Design of Tubular Structures, Tokyo, July.

Key, P.W., Hasan, S.W. and Hancock, G.J. (1988), "Column Behaviour of Cold–Formed Hollow Sections", J. Struct. Eng., ASCE, Vol. 114, No. ST2, Feb., pp390–407.

Little, G.H. (1977), "Rapid Analysis of Plate Collapse by Live Energy Minimisation", Int. J. Mech. Sci, Vol 19, pp725–744.

Mendelson, A. (1968), Plasticity: Theory and Applications, The Macmillan Company, New York, 1968.

Mofflin, D.S. (1983), "Plate Buckling in Steel and Aluminium", PhD Thesis, University of Cambridge, August.

Moxham, K.E. (1971), "Theoretical Determination of the Strength of Welded Steel Plates in Compression", Report, University of Cambridge, Department of Engineering, No. TR2.

Moxham, K.E. (1970), "Compression in Welded Web Plates", PhD Thesis, University of Cambridge, June.

Scaramangas, A. (1984), "Residual Stresses in Girth Butt Welded Pipes:– Experimental Techniques", Technical Report, CUED/D–Struct/TR.108, Cambridge University.

Sridharan, S. and Graves–Smith, T.R. (1981), "Postbuckling Analysis with Finite Strips", J. Eng. Mech Div., ASCE, Vol. 107, pp869–888, October.

Sridharan, S. (1982), "A Semi–Analytical Method for the Post–Local–Torsional Buckling of Prismatic Plate Structures", Int. J. Num. Methods Eng., Vol. 18 pp 1685–1697.

Timoshenko, S.P. and Woinowsky–Krieger, S. (1959), Theory of Plates and Shells, McGraw–Hill Book Co., Inc., New York, N.Y.

Yamaki, N. (1959), "Postbuckling Behaviour of Rectangular Plates with Small Initial Curvature Loaded in Edge Compression", Journal of Applied Mechanics, ASME, Sept., pp 407–414.

8. APPENDIX II NOTATION

b	Width of strip
b_f, b_w	Width and depth of box section
f_u, f_v, f_w	Polynomial functions of y alone
L	Length of Strip
m	Secondary displacement harmonic number
n	Primary displacement harmonic number
u,v,w	Displacements in x,y,z directions respectively
w_0	Plate geometric imperfection
x,y,z	Cartesian coordinates
$_m\gamma_{xy}$	Membrane shear strain in x,y plane
γ_{xy}	Shear strain in x,y plane
$\Delta\epsilon_x{}^p, \Delta\epsilon_y{}^p, \Delta\gamma_{xy}{}^p$	Plastic strain increment
$_m\epsilon_x, _m\epsilon_y$	Membrane strain in x,y directions
ϵ_x, ϵ_y	Strain in x,y directions
ϵ_Y	Yield strain
ν	Poisson's ratio
$\sigma_x, \sigma_y, \sigma_z$	Longitudinal stress in x,y,z directions
τ_{xy}	Shear stress in x,y plane
σ_e	Von Mises effective stress
σ_m	Mean compressive stress
σ_{cr}	Elastic critical stress
σ_R	Residual stress
σ_{ult}	Ultimate stress
σ_Y	Yield stress

(a) Simply-Supported Plate

(b) Outstand

(c) Channel Section

(d) I-Section

(e) Fabricated Hollow Section

(f) Cold-Formed Hollow Section
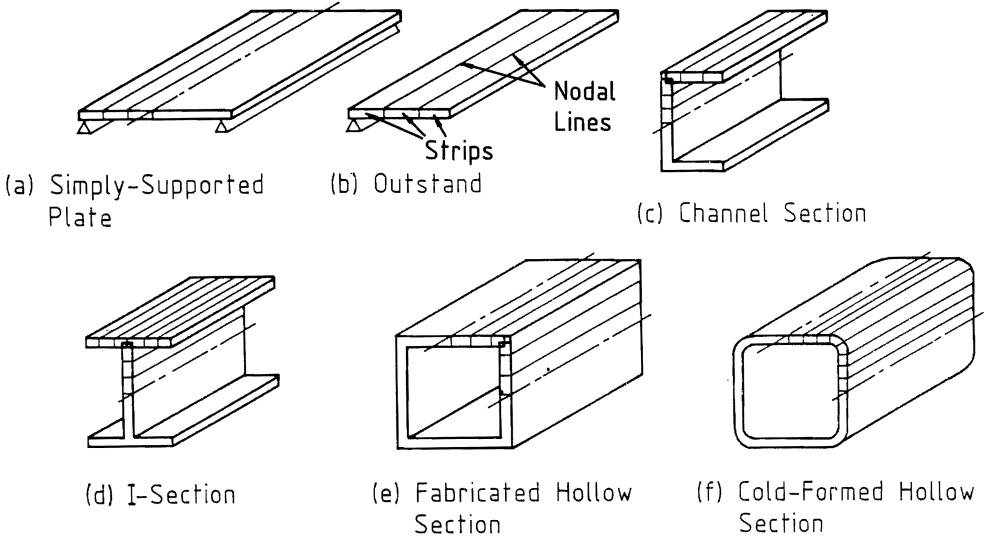
FIG.1 TYPICAL MEMBER FINITE STRIP SUBDIVISION
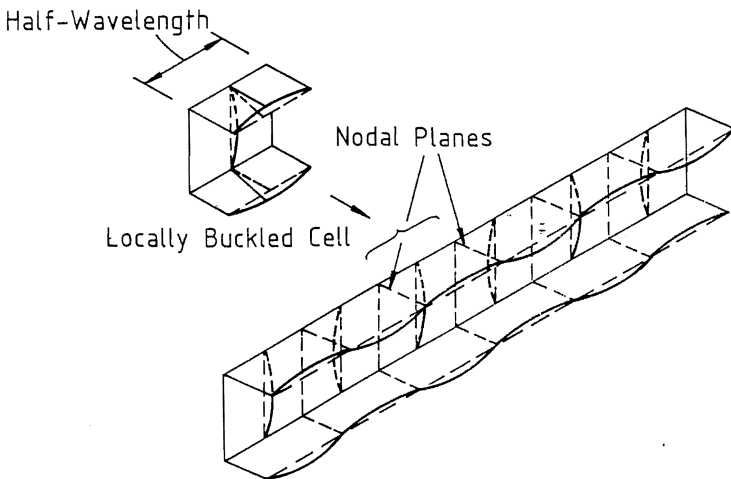
FIG.2 LOCALLY BUCKLED MEMBER

89
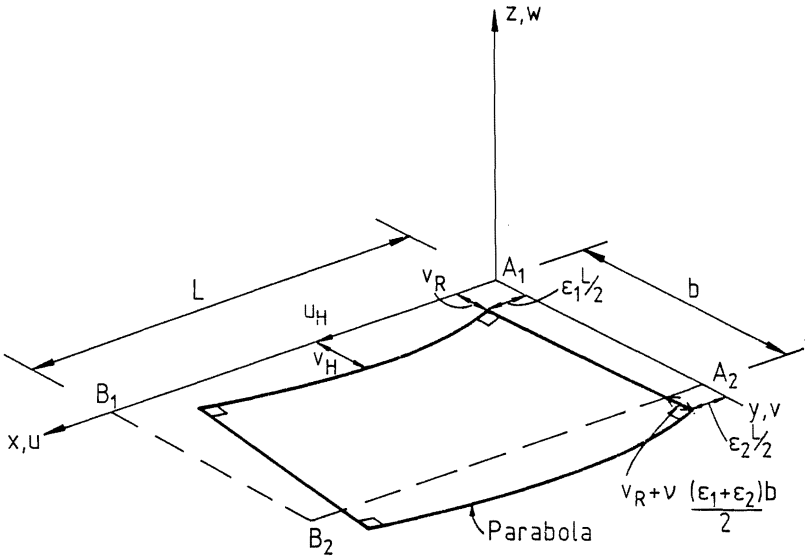
FIG.3 FINITE STRIP COORDINATE SYSTEM AND PREBUCKLING
DISPLACEMENT FIELD
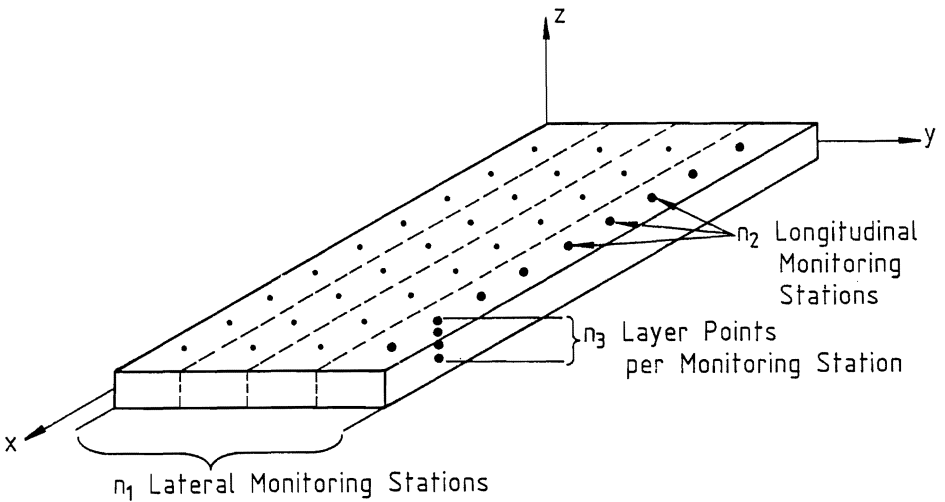
FIG.4 FINITE STRIP INTEGRATION TERMINOLOGY
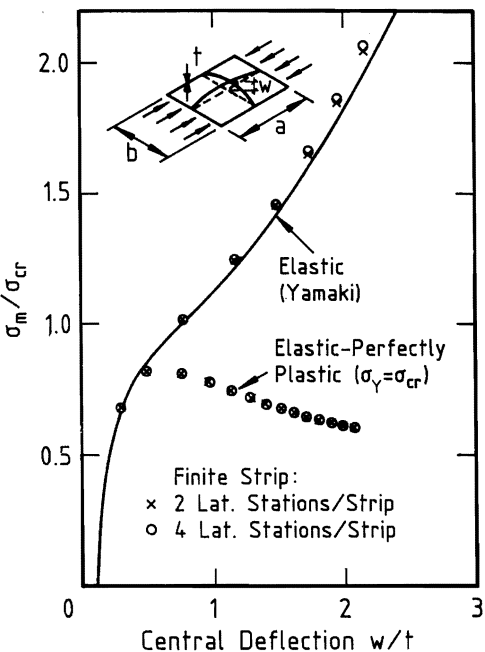
(a) Effect of Number of Lateral
   Monitoring Stations (n_1)
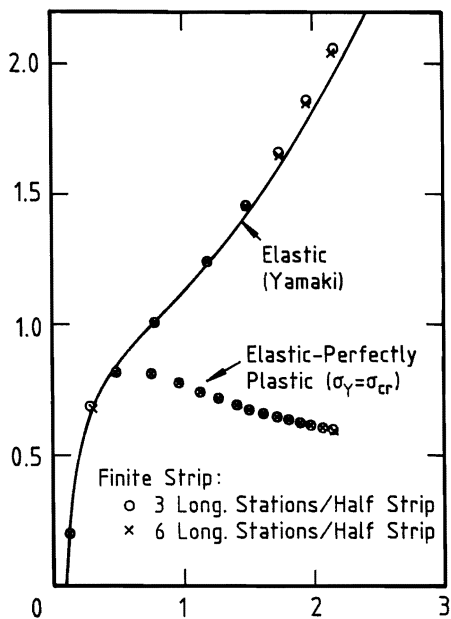
(b) Effect of Number of Longitudinal
   Monitoring Stations (n_2)
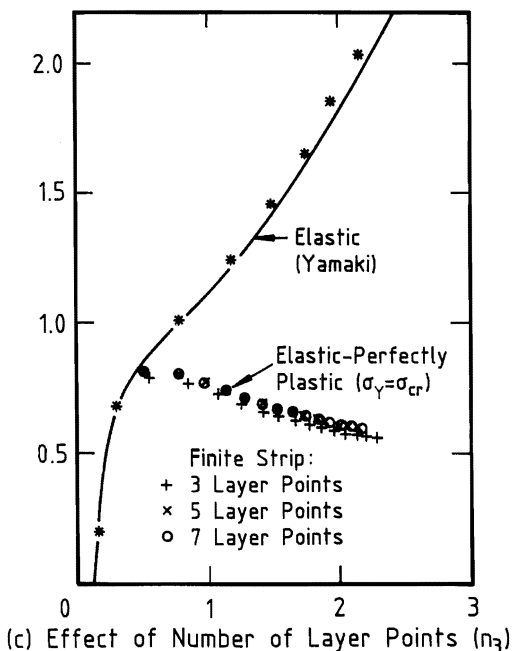
(c) Effect of Number of Layer Points (n_3)
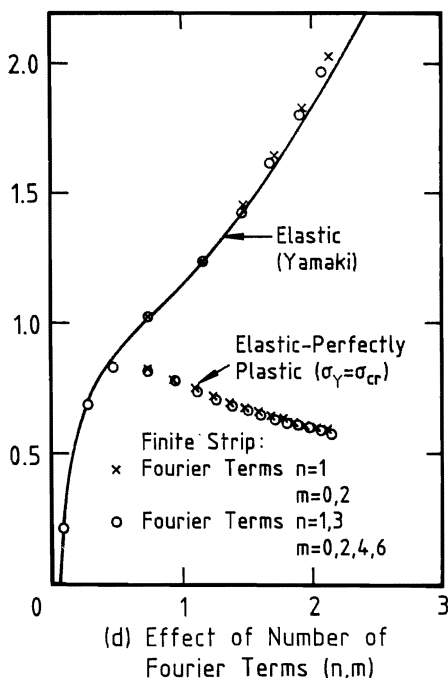
(d) Effect of Number of
   Fourier Terms (n,m)

FIG.5   INVESTIGATION OF FINITE STRIP PROGRAM PARAMETERS
        SQUARE PLATE (a/b=1.0), $w_0/t=0.1$
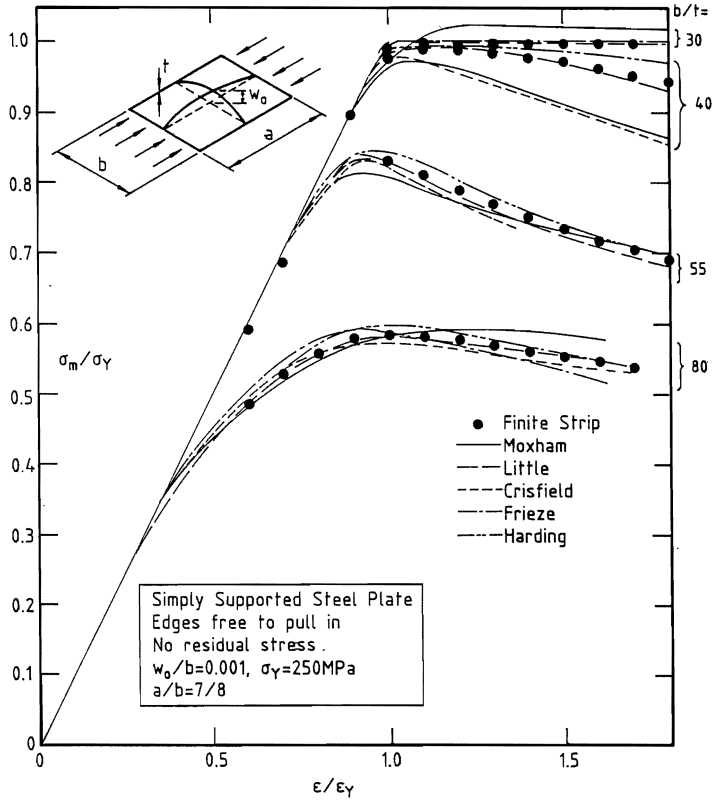
FIG.6 PLATE LOAD-SHORTENING CURVES
COMPARISON WITH FINITE STRIP
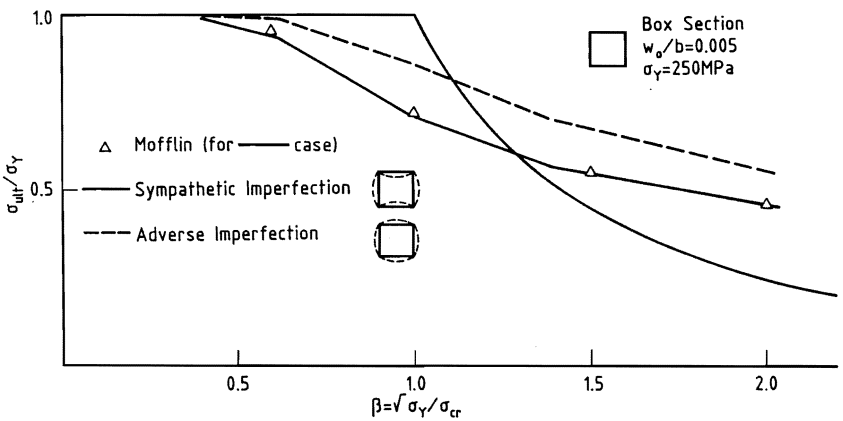
FIG.7 ULTIMATE STRENGTH CURVES
BOX SECTION (b$_w$/b$_f$=1.0)

(a) Panel Removal

Released Residual Stress
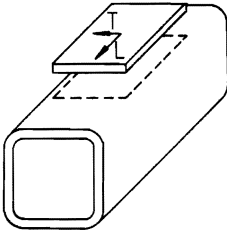
(b) Small Block Removal
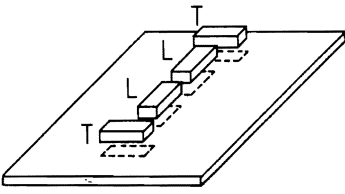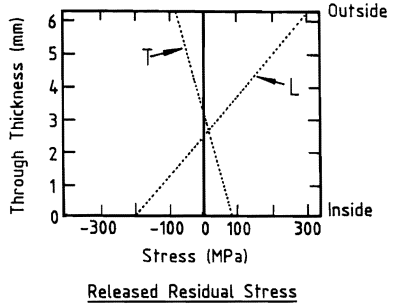
Released Residual Stress
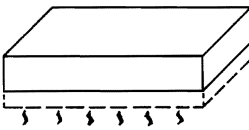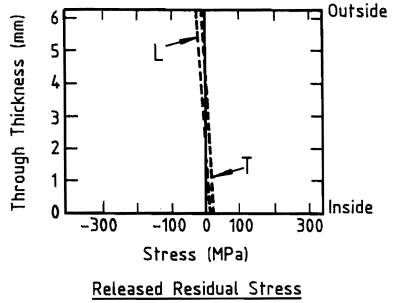
(c) Small Block Spark
Erosion Layering
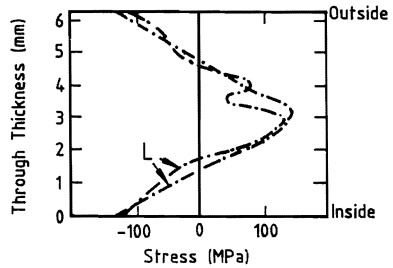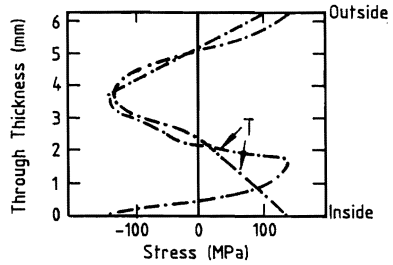
Note: +ve Stress is Tensile
T=Transverse Measurement
L=Longitudinal Measurement

Released Residual Stress

FIG.8   EXPERIMENTAL DETERMINATION OF THROUGH THICKNESS
RESIDUAL STRESS (254×254×6.3 SHS)
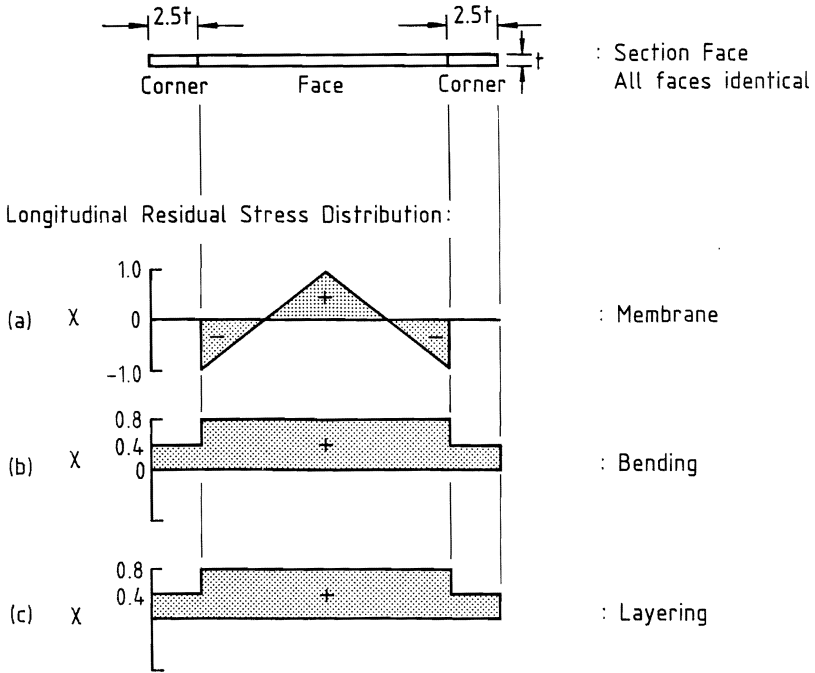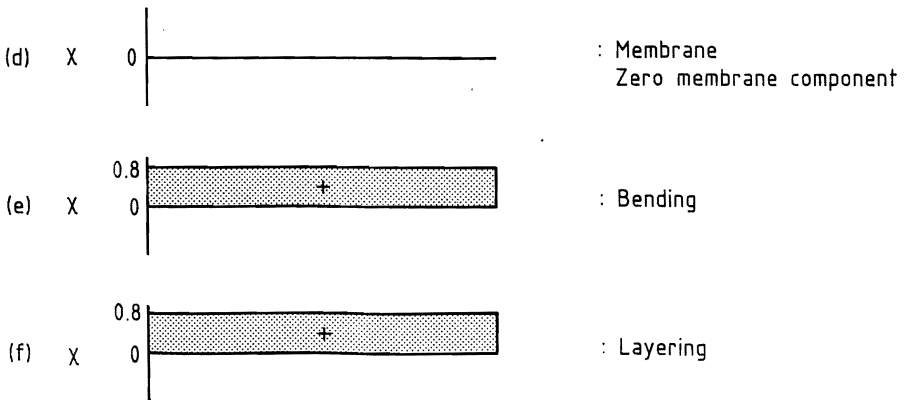
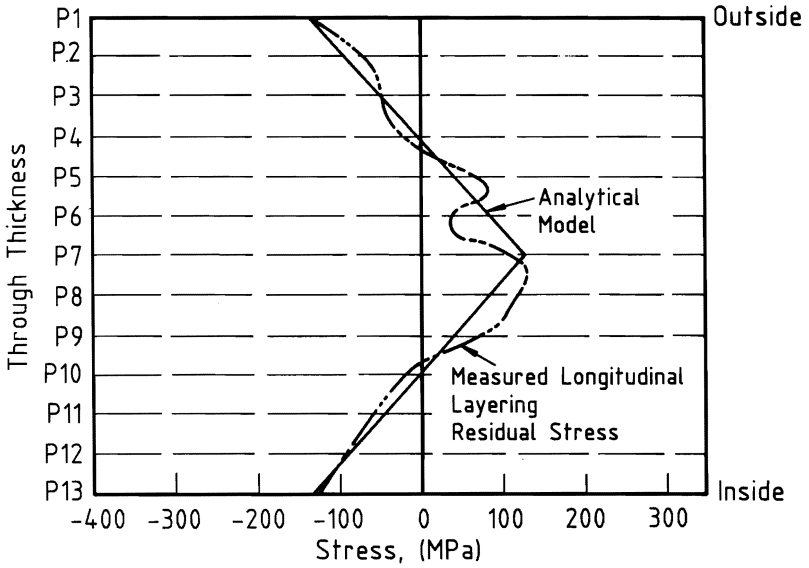FIG.9 ANALYTICAL MODELS OF RESIDUAL STRESS
DISTRIBUTIONS ACROSS FACES
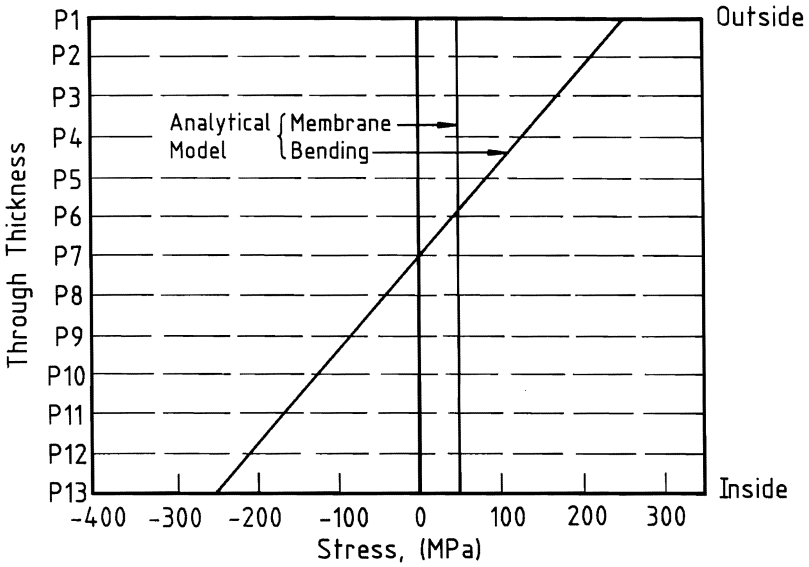
(a) Longitudinal Residual Stress. (σ_R)
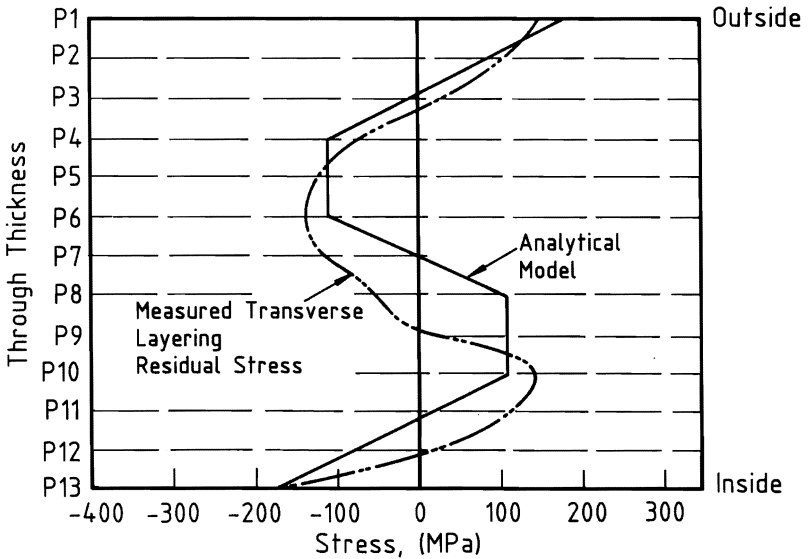+ve Tensile Stress
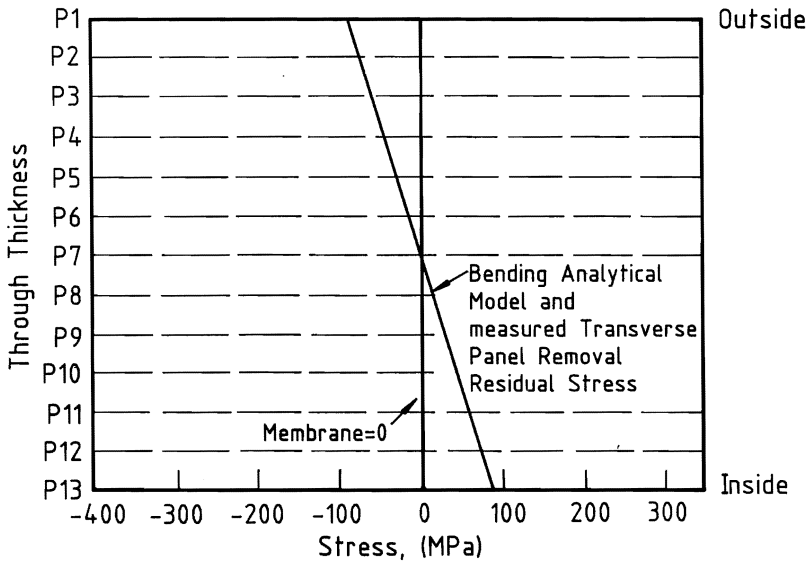
(b) Transverse Residual Stress (σ_R)
+ve Tensile Stress

FIG.10   ANALYTICAL MODELS OF PANEL REMOVAL
RESIDUAL STRESS

(a) Longitudinal Residual Stress (σ_R)
+ve Tensile Stress

(b) Transverse Residual Stress (σ_R)
+ve Tensile Stress

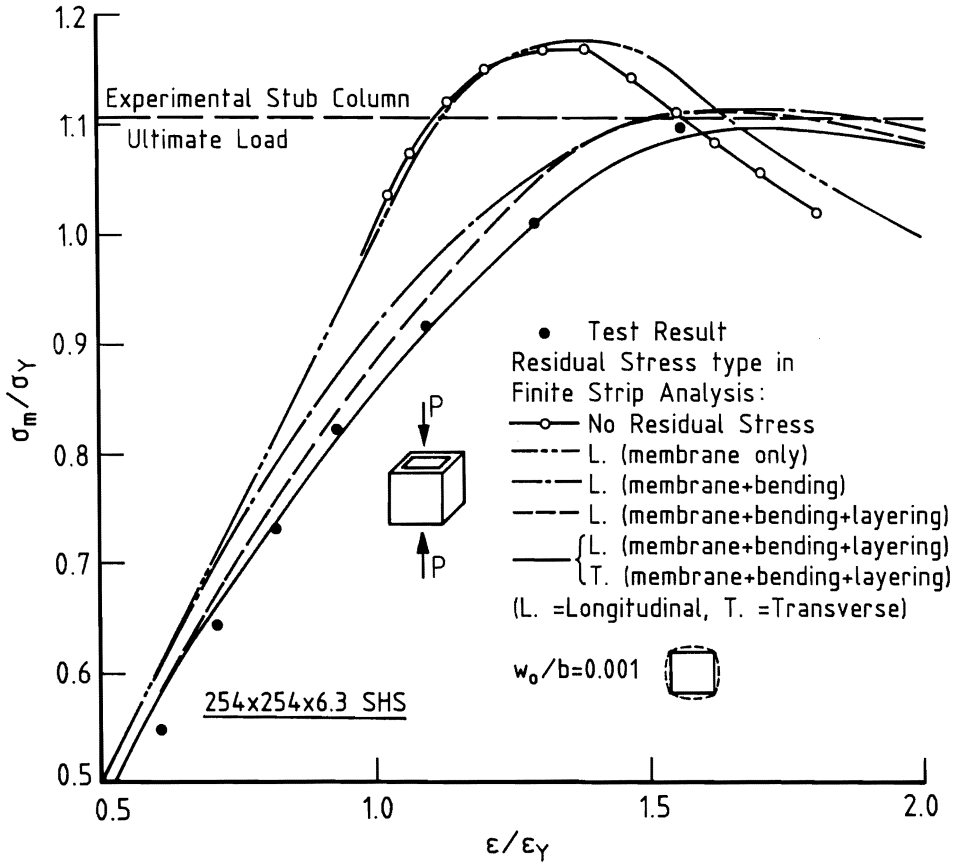FIG.11 ANALYTICAL MODELS OF LAYERING
RESIDUAL STRESS

FIG.12   STRESS VERSUS AXIAL STRAIN
254x254x6.3 SHS STUB COLUMN
INFLUENCE OF RESIDUAL STRESS